Analyst

Accepted Manuscript

ROYAL SOCIETY OF CHEMISTRY

www.rsc.org/analyst

Journal Name

RSCPublishing

ARTICLE

Novel screening method of oxidation and reduction abilities for photocatalytic materials

Cite this: DOI: 10.1039/xoxxooooox

K. Katayama,[a] Y. Takeda,[a] K. Shimaoka, [a] K. Yoshida,[a] R. Shimizu, [a] T. Ishiwata, [a] A. Nakamura, [a] S. Kuwahara, [a] A. Mase, [b] T. Sugita, [b] M. Mori [b]

Received ooth January 2012,
Accepted ooth January 2012

DOI: 10.1039/xoxxooooox

www.rsc.org/

Two analytical methods for evaluation of photocatalytic oxidation and reduction abilities were developed using a photocatalytic microreactor; one is the product analysis and the other is the reaction rate analysis. Two simple organic conversion reactions were selected for the oxidation and reduction, respectively. Since the reactions were one-to-one conversion from the reactant species to the product species, the product analysis was simply made by gas chromatography, and the reactions were monitored in-situ in the photocatalytic microreactor by the UV absorption spectrum. The partial oxidation and reduction abilities for each functional group can be judged from the yield and selectivity of the product analysis, and the corresponding reaction rate, while the ability of the total oxidation can be judged from the conversion of each reaction in the product analysis. We demonstrated the application of these methods for several kinds of visible photocatalysts.

Introduction

Photocatalytic materials, based on titanium oxide (TiO_2), have been commercialized for the purpose of self-cleaning of walls of houses, toilets, interior walls in tunnels, etc. In principle, by irradiating a light to a photocatalyst, hydroxyl radical is generated by the oxidation of water, and super oxide anion is generated via the reduction of oxygen under aqueous or ambient conditions, and the active species are in an equilibrium with water, and hydrogen peroxide is generated. Such active species are called active oxygen species (AOS), and they induce the photocatalytic degradation of organic molecules. They are also subject to degradation due to direct oxidization by the holes generated in photocatalysts at their surface.[1]

In most of the applications using photocatalytic reactions, only the oxidation ability, especially total oxidation from organics to carbon dioxide and water, has been paid attention to. However, photocatalyst also has the abilities such as partial or selective oxidation,[2-7] and reduction [8-10] for various aromatic compounds.[11, 12]. Selective oxidation of the alcohol functional group gave a high yield.[13] The reduction of nitrocompounds was investigated well on the reaction mechanism.[8, 14, 15] and imine formation was reported after reacting with alcohols.[16] Furthermore, complicated reactions following the photocatalytically generated intermediate radical species were found, too.[5, 17, 18]

In recent years, the demand for the visible light response has been increasing, and many papers on the development of new materials have been reported. This is not only for the organic decomposition, but also the generation of solar fuels and light harvesting applications.[19-21] Although the development of materials has been intensively expanding, the analytical methods for understanding the ability of the materials have been unchanged. Typical examinations for the photocatalytic materials are the color degradation of methylene blue in aqueous solutions [22, 23], decomposition of acetaldehyde under ambient condition,[24] defined in the Japanese Industrial Standard (JIS). These methods give an information on the ability of total oxidization. There is another promising method, where the oxidization of dimethylsulfoxide is observed by ion chromatography.[25] Since methyl groups are replaced with hydroxyl radicals step by step, the obtained products reflect direct information on the hydroxyl radical activity.

From our point of view, the analytical methods for photocatalysts are not sufficient to cover many recently developed materials, which may have another potential application. The problems for the conventional analytical methods are in the following; 1. Under aqueous or ambient conditions, various AOSs depending on the experimental conditions (pH, humidity, coexisting species) are involved in the photodecomposition, and it is difficult to assign which one is the actual cause for the reaction, 2. Dye degradation such as methylene blue is not a good test material because it is subject to multi-point reactions in the molecule at the same time as we clarified in the previous study,[26] and the color degradation does not necessarily reflect the ability of the total oxidation.

We recently developed a spectroscopic monitoring system for photocatalytic reactions using a microreactor[26] to reduce the reaction time, and successfully accomplish a quick monitoring of a photocatalytic reaction in a capillary. There are also several reports on the decrease in the reaction time by utilizing microreactors in the

photocatalytic reactions.[27-32] We studied the reaction mechanisms for various dyes composing of different main structures, and we successfully made a kinetic analysis and clarified multi-step reactions, self-catalytic reactions, and further complicated reactions by monitoring the intermediate species involved in each reaction. The result suggested that typical analyses based on the quasi-first-order or Langmuir Hinshelwood mechanisms [33, 34] are not enough to clarify the reaction processes correctly. Furthermore, we proposed a new concept of a photocatalytic microreactor, where no electrical resources are necessary to perform the photocatalytic reaction by using a natural force such as capillary force and diffusion due to concentration gradient, and successfully demonstrated it in the previous paper.[35]

In this study, we propose a new methodology, so that we can clarify the actual abilities of photocatalytic materials, by obtaining the abilities of the selective oxidation and reduction and the total oxidation, and the corresponding reaction rate by using simple screening methods by using a photocatalytic microreactor. We selected some of the oxidation and reduction reactions in organic solvents, not in water to avoid the complexity of the reactions involving various AOSs. By the analysis of the simple oxidation and reduction reactions, the ability of electron or hole donation can be understood. We applied two methods for these reactions; one is the product analysis to know the conversion, yield and selectivity, giving information on the abilities of the total oxidation, partial oxidation and reduction, and the other is the reaction rate analysis by monitoring the reaction directly inside the microreactor with a UV spectrum.

Experimental

In the product analyses, photocatalytic reactions were performed using the automatic photocatalytic reactors we developed in the previous paper.[35] Briefly, the principle is explained in the following. (Fig.S1) Photocatalytic microreactors were prepared by coating photocatalytic materials inside a capillary with both ends open. Six capillaries are bundled and the bottom is soaked in a reagent solution in a test tube. Due to the capillary force, the solution is sucked up to a height on the order of several centimeters, where UV or visible light is irradiated to proceed the reaction. Since the reactant is decomposed by light irradiation, a concentration gradient is formed inside the microreactors, driving the reactants beneath the capillary bundle into the microreactors due to diffusion, and vise versa for the products. The reaction then continues until the concentration gradient disappears; thus, all of the reactants are decomposed.

The photocatalyst was coated inside a fused silica capillary (I.D. 1.1 mm, O.D. 1.4 mm) with a length of 6 cm. The capillary was transparent, and was treated using an alkaline solution before coating. The capillary was soaked in each paste and the inside was filled with the solution three times, and furnaced at 450 ^{o}C for 1 hr. Six capillaries were bundled, and were placed in a test tube, including a reactant solution (1 mL). Due to the capillary forces, the reactant solution typically rose up a few centimeters above the solution surface.

The test tubes were loaded on a merry-go-round type photoreaction stage with 8 test tube holders (Fig. S2), and a light was shone from the side with a distance about 10 cm for typically 18 hrs. The reaction time was decided in advance by checking the necessary reaction time for 1-mL reactant solution with 6 photocatalytic microreactors. A UV-LED with a wavelength of 365 nm and the intensity of 360 mW/cm^2 was used as a UV source, and a quasi sunlight source (XC-100, Solax) was used as a visible light source. After the reaction, the solution was analysed by gas chromatography (Shimadzu, GC-2014) and GC mass spectrometer (Agilent, 6890N(GC), 5975B (inert XL El/Cl MSD)).

For the reaction rate analysis, the reaction monitoring system was used (Fig. S3), which was developed in the previous paper for the study on the dye degradation processes.[26] Some revisions were made to measure the UV spectrum of simple organic molecules. The light source was a deuterium lamp (D2) and UV spectrometer (Ocean optics, USB4000) covering the wavelength range from 220 – 400 nm. The capillary used for the photocatalytic microreactor was made of fused silica with 500 micrometer in diameter.

The solution was injected into the capillary using a syringe pump. After the flow was stopped, we waited for ca. 30 seconds until adsorption equilibrium was reached. The photocatalytic reaction was initiated by the light irradiation from the top side. The light was a UV-LED at 365 nm for UV photocatalysts and a one at 450 nm for visible photocatalysts. Perpendicularly with the light, a fiber tip connected with the D2 lamp was placed at the reaction location. The other end of the fiber tip was placed on the opposite side of the D2 lamp irradiation, and the absorption spectrum was monitored with a spectrometer. The intensity of the D2 lamp was adjusted not to induce photoreaction or photocatalytic reaction.

As a typical photocatalyst, TiO_2 powder (P25, average diameter(D): 21 nm) was used. It was mixed with water (3.33 mL) and acetylacetone (0.33 mL) and mixed in a mortar for 30 min, to prepare a TiO_2 paste. As a visible photocatalyst, a tungsten oxide coating solution (Toshiba materials, SJ9003-1, D: ca. 100 nm), nitrogen doped titanium oxide (N-TiO_2, D: 22 nm), N-TiO_2 doped with silicon, which is effective to reduce the defects in TiO_2 (N-Si-TiO_2, D: 11 nm), N-Si-TiO_2 deposited with vanadium (V-N-Si-TiO_2, D: 13 nm), [36, 37] which was reported for enhancement of photocatalytic ability, were used. Powder samples were dispersed in a solution by the same method as for the TiO_2 powder to prepare a paste. The method for the paste preparation is a general procedure for coating a nanoparticulate inorganic material on a glass. It was confirmed that the thickness of the coating was 3∓0.5 micron for any materials used here, but the porosity was ranged from 40-60 %.

We investigated organic conversion of various molecules due to photocatalytic reactions, and we selected the following reactions as candidates to show the abilities of oxidation and reduction. To select the reactions, we put an importance on the simplicity of the reaction, easy monitoring in the UV spectrum for the reactant and product.

Oxidation

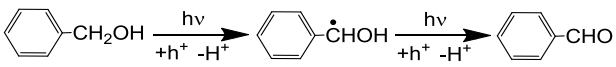

(1)

Reduction

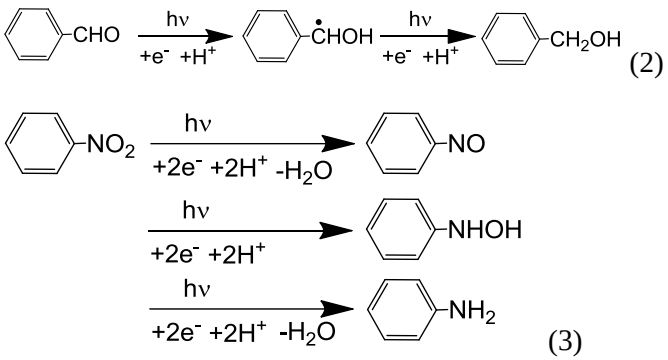

Scheme Reaction candidates for the photocatalytic oxidation and reduction.

Oxidation of benzylalcohol (BAlc)to benzaldehyde (BAld),[2, 5] and reduction of BAld to benzyl alcohol were selected and the reaction schemes are shown in Scheme (1) and (2). They are the reverse reactions each other, and they can be controlled just by changing the solvent; acetonitrile for oxidation and ethanol for reduction. In the oxidation, holes are used as an oxidant. In the reduction, since ethanol is a good scavenger of photoexcited holes, which prevents the recombination of electrons, the electrons were used for reduction. [14, 38] Initially, we picked up these reactions because the product analyses by GC and the spectrum monitoring were easy because we have only to monitor the BAlc and BAld. However, we selected another reduction reaction, the reduction of nitrobenzene (NB) to aniline (AN) (Scheme (3)), [8, 14, 15] due to several reasons as we will explain in the following section.

Results and Discussions

1. Product analysis

In case of a typical photocatalyst, TiO_2, the GC charts before and after the reactions for the oxidation of BAlc and the reduction of BAld and NB are shown in Fig.1. The initial concentrations of the reactant solutions were 1 mM. In Fig.1, all the peaks for the reactants were decreased after the reaction. In the oxidation reaction, only the peak for BAld at 21 min was observed as product species, except the solvent peak. In the reduction reactions, the peaks for the corresponding reduced species, BAlc at 32 min was observed and several other peaks were observed, which corresponds to the acetaldehyde and acetic acid peaks due to the oxidation of ethanol. Since we did not observe any peaks except the products and the solvent origin, no by-products were observed, and we can predict that the rest of the products would be carbon dioxide and water. In case of the reduction of NB, the peaks for aniline (AN) at 7.8 min and nitrosobenzene at 6.5 min were observed, and the latter is an intermediate species. In this reaction, light irradiation was only 30 min because unknown reactions proceeded for the longer irradiation time.

The conversion, yield, and selectivity were summarized in Table 1. The conversion value can be utilized as a guide for the estimation of how efficiently the photoexcited electrons and holes were utilized, namely the total oxidation ability. The selectivity and yield are

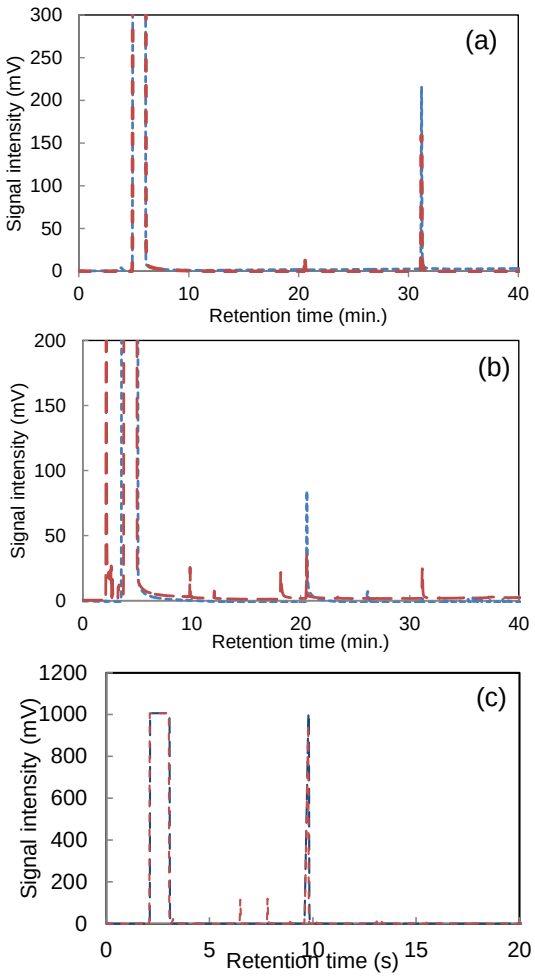

Fig. 1 The GC charts before and after photocatalytic reaction of (a) oxidation of benzylalcohol, (b) reduction of benzaldehyde, (c) reduction of nitrobenzene. Dot line and long dot line corresponds the ones before and after the reaction. The reaction time for (1) and (2) was 18 hrs, and 30 min for (3).

indicators for how much of them were used for the intended reactions.

Table 1 Conversion, yield and selectivity for the oxidation and reduction reactions in the photocatalytic microreactor; (1) oxidation of benzyl alcohol, (2) reduction of benzaldehyde, (3) reduction of nitrobenzene. The reaction time for (1) and (2) was 18 hrs, and 30 min for (3).

Entry	Conversion (%)	Yield (%)	Selectivity (%)
(1)	24	8	33
(2)	69	23	33
(3)	6	5	77

2. Reaction rate analysis

Each reaction was monitored in-situ by UV absorption spectrum.

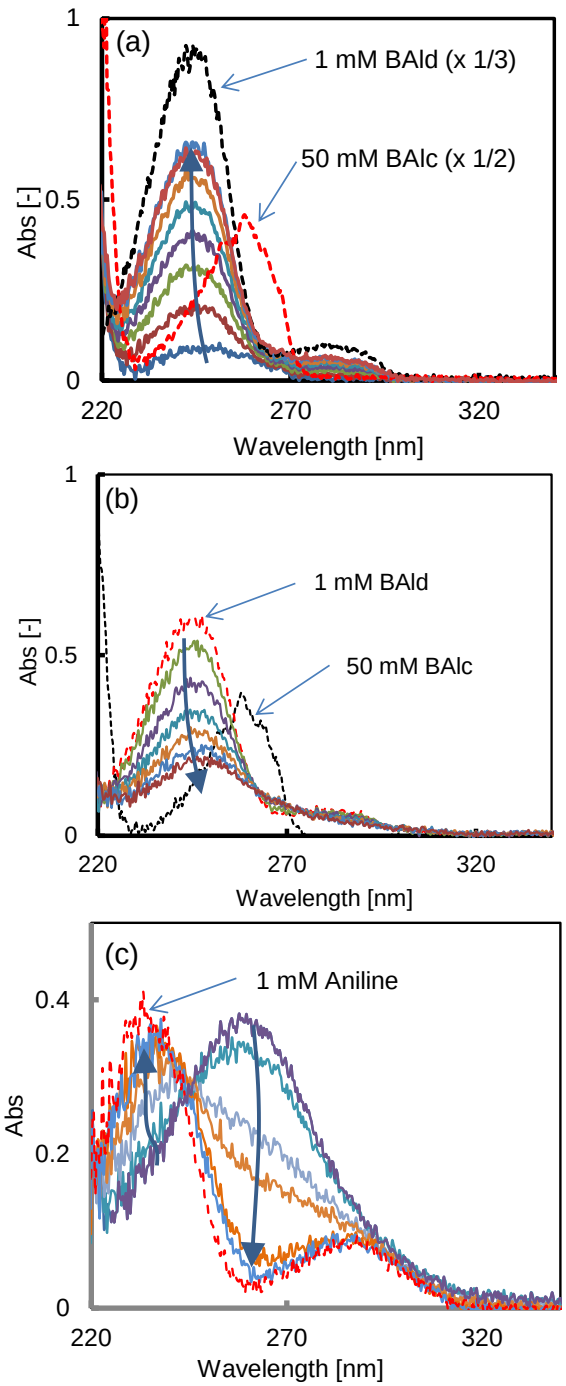

Fig.2 Absorption spectra for the oxidation and reduction reactions observed directly in a photocatalytic microreactor; (a) corresponds for the oxidation of benzylalcohol. The spectra for 0, 10, 20, 30, 40, 50, 60, 80 s after the reaction was started by UV irradiation were shown. The dotted lines indicate the reference spectra for benzylalcohol and benzaldehyde. (b) corresponds for the reduction of benzaldehyde. The spectra for 0, 80, 100, 120, 140, 160, 175 s after the reaction started were shown. The dotted lines indicate the reference spectra for benzylalcohol and benzaldehyde. It is noted that the absorbance were different in (a) and (b) because of the solvent difference. (c) corresponds for the reduction of nitrobenzene. The spectra for 0, 20, 40, 60, 80, 100 s after the reaction started were shown. The dotted line indicates the reference spectrum for aniline.

The temporal changes in the spectra for the oxidation and reduction reactions were shown in Fig.2. In the oxidation reaction, 5 mM BAlc/ACN was used as a reactant, and the spectrum for BAlc peaked at 270 nm gradually decayed and changed into the spectrum for BAld. It is noted that the reaction was almost saturated about 60 s. From the reference spectra for BAld and BAlc in ACN at certain concentrations, we could fit each spectrum during the reaction by the summation of these reference spectra, and we could obtain the concentrations of BAld and BAlc at each time. (A typical fitted spectrum is shown in Fig. S4.)

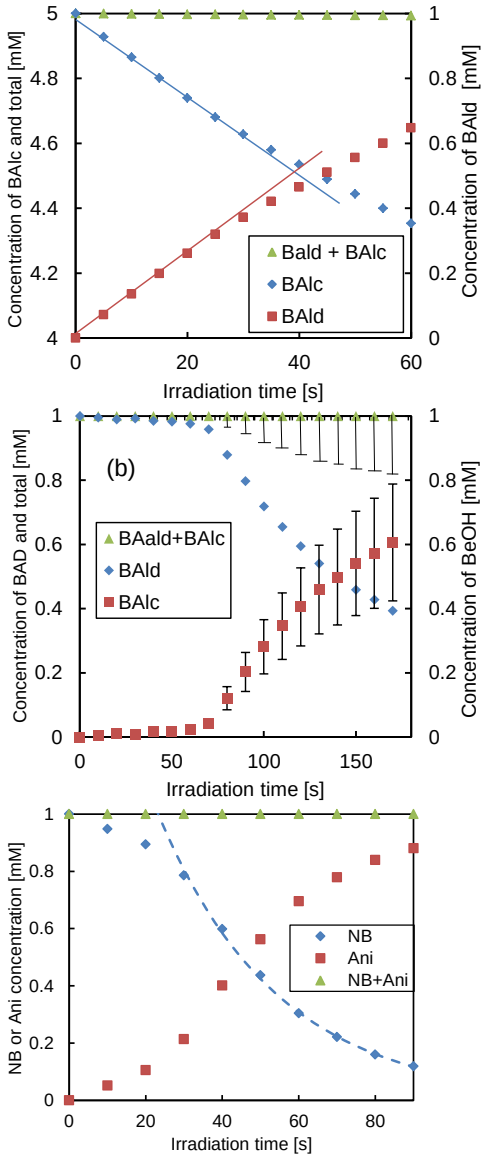

Fig.3 Temporal change of the reactant and product concentration in the oxidation and reduction reactions in the photocatalytic microreactors; (a) the oxidation reaction of benzyl alcohol. (b) the reduction reaction of benzaldehyde. (c) the reduction reaction of nitrobenzene. Fitting curves for BAlc and BAld in (a) and for NB in (c) are shown by the analysis of the 0^{th} order and 1^{st} order kinetics.

The concentration change during the reaction was shown in Fig. 3. A concentration increase in BAld and a decrease in BAlc were confirmed and the change was gradually saturated about 60 s. It is noted that the sum of BAld and BAlc concentrations remained 5

mM. It indicated that this reaction proceeded with 100 % selectivity until 60 seconds after the reaction started. We suppose that the reason why the reaction was saturated is because the product species covered the active reaction sites, because the reactivity was recovered by the replacement of the solution.

Furthermore, the concentrations for BAld and BAlc showed a linear change with time, and it indicated that this reaction is on the zeroth order, which can be explained by the rate analysis of the surface reaction. (See Appendix) Since the reaction was saturated as the reaction proceeded, the straight part of the concentration change was used to analyse the data. We could successfully obtain the reaction rate constant, 0.011 (mol/l· s).

Similarly, the reduction of BAld was monitored as shown in Fig.2(b). The reduction did not proceed about 60 s after the photoirradiation, and BAld suddenly decreased after that. We tried fitting of the spectrum similarly as the case for the oxidation reaction, but it was very difficult to obtain the exact concentration of BAlc because the absorption intensity for BAld is much stronger than BAlc for the same concentration, and the contribution of BAlc in the spectrum was difficult to be deduced, and the error was very large for the BAlc concentration for the smaller concentrations of BAlc, shown in Fig.3(b). (It is reminded that the absorbance for BAld and BAlc were different because of the solvent difference in Fig.2(a) and (b).) Since it is still unclear why there was a lag time for the starting of the reaction and also the accuracy of the BAlc concentration was not good enough, we selected another reaction for the reduction reaction.

Then, we used a conversion reaction from NB to ANI, which is a well-known reduction reaction using photocatalysis. The peak at 270 nm, correspoinding to NB, gradually decayed and a new peak at 250 nm grew up, and the reaction was saturated around 100 s. However, the spectrum for the product did not perfectly match that for ANI, which has a peak around 240 nm.

We suspected that ANI was subject to photoreaction, and thus the spectrum change of ANI by irradiation of UV light was monitored. Actually the spectrum shifted from 240 to 250 nm in its peak and the corresponding spectrum agreed well with the product spectrum for the NB reduction. The product was an imine compound, confirmed from the GC-MS analysis (N-Ethylideneaniline). Thus, it is considered that ANI was generated by the reduction of NB but that the generated ANI was changed into the imine compound by reacting with acetaldehyde generated via the oxidation of ethanol.

However, we found out that ANI did not react in 2-propanol as a solvent, probably because the oxidized molecule, acetone do not react with ANI. The reduction of NB in 2-propanol is shown in Fig.2(c), and we could successfully observe the pure reduction reaction from NB to ANI. The spectrum during the reaction was fully fitted with the summation of ANI and NB spectra.(Fig.S4(c)) The concentration change during the reaction is shown in Fig.3(c). We observed 10-20 seconds for starting the reaction, which was much shorter than that for the reduction of BAld, and the lag time was reproducible as long as TiO_2 was used. Neglecting the lag time, the concentration change follows the 1st order reaction as shown in Fig.3(c), and the reaction rate was obtained as 0.032 (/s). (It is noted that this value is the multiplication of the reaction rate and the adsorption equilibrium constant. See Appendix.)

3. Application of the screening methods for the visible photocatalysts

The evaluation of several visible photocatalysts by using the oxidation and reduction reactions was made. The following photocatalysts were analysed; WO_3, N-TiO_2 as typical visible photocatalysts, N-TiO_2 doped with silicon, which is effective to reduce the defects in TiO_2 (N-Si-TiO2),[36] N-Si-TiO_2 deposited with vanadium (V-N-Si-TiO2), which was reported for enhancement of photocatalytic ability.[37]

The result for the oxidation reaction of BAlc is shown in Table 2. The comparison result for TiO_2 under UV irradiation with similar light intensity was shown too. Overall, the oxidation ability of visible photocatalysts showed a comparable level as that for TiO_2 under UV illumination, considering the differences of the light intensity and absorbance of materials, etc. WO_3 showed the highest conversion but the selectivity was quite low. With regard to the Si doping, N-Si-TiO_2 showed higher conversion and selectivity compared with N-TiO_2. Vanadium deposition gave a lower efficiency for the oxidation. The result for the reduction reaction of BAld is shown in Table 3. Compared with TiO_2, the reduction ability for the visible photocatalyts was quite low as a whole, and no reduction product was observed for WO_3, which can be explained by the low conduction band position. In the visible photocatalyts, N-Si-TiO_2 showed the highest conversion and selectivity, and vanadium deposition lowered the reaction efficiency.

Table.2 Conversion, yield and selectivity for the oxidation of benzylalcohol in the photocatalytic microreactor for various photocatalytic materials.

Entry	Conversion (%)	Yield (%)	Selectivity (%)
TiO_2 with UV	17	3.7	22
WO_3	25	0.3	1.0
N-TiO_2	7.5	3.7	49
N-Si-TiO_2	14	8.1	56
V-N-Si-TiO_2	8.8	5.6	56

Table.3 Conversion, yield and selectivity for the reduction of benzylaldehyde in the photocatalytic microreactor for various photocatalytic materials.

Entry	Conversion (%)	Yield (%)	Selectivity (%)
TiO_2 with UV	51	17	17
WO_3	8.3	0	0
N-TiO_2	14	2.4	17
N-Si-TiO_2	18	5.2	29
V-N-Si-TiO_2	12	1.6	13

The reaction rate analysis was made for the visible photocatalyts. Since they showed very low reduction ability, we studied only the BAlc oxidation reaction, which proceeded with almost 100 % selectivity even for the visible photocatalysts. The temporal change in the reactant and product concentrations are shown in Fig. S5 in Supporting Infromation. The obtained reaction rates are listed in Table 4.

Table.4 Reaction rate for the BAlc oxidation measured by the direct UV monitoring in the photocatalytic microreactor.

Entry	Conversion reaction rate (x10 $^{-3}$ mol/l· s)
WO_3	0.440
N-TiO_2	0.298
N-Si-TiO_2	0.214
V-N-Si-TiO_2	0.160

From the product analysis and reaction rate analysis, the oxidation ability for WO_3 was high, although the reaction was not selective. There was a discrepancy between the product analysis and reaction rate analysis on the oxidation ability between N-TiO_2 and N-Si-TiO_2. This is probably because N-TiO_2 lost the reaction ability during the long reaction time, while the initial reaction rate was large during the reaction rate analysis within a few minutes. Basically, it can be said that Si doping in TiO_2 is effective to enhance both the oxidation and reduction reactions due to the decrease in the internal defects. But we could not confirm the enhancement of the reaction efficiency by the vanadium deposition, because both the oxidation and reduction reactions were deactivated. This is probably because the deposition would reduce the active reaction site.

Conclusion

We developed two analytical methods for evaluation of photocatalytic materials using a photocatalytic microreactor; one is the product analysis and the other is the reaction rate analysis. To make a simple analysis for the photocatalytic ability, we selected oxidation and reduction reactions of organic conversion reactions, which are easily monitored by GC and absorption spectrum due to one-to-one reactions. We could establish the method for product analysis and reaction rate analysis, and they were applied to several visible photocatalysts. It is expected that this novel analytical procedure for various photocatalytic materials accelerate the development of new materials which is really useful for each purpose.

Appendix

The case when the reaction order is zeroth and first order is explained by the analysis of the rate equation for the surface reaction. When we think about the following reaction at the surface,

$$A + \sigma \underset{k_A'}{\overset{k_A}{\rightleftarrows}} A\sigma \quad (1)$$

$$A\sigma \xrightarrow{k_r} C\sigma \quad (2)$$

, where A and C are the reactant and product, respectively, and σ is the active reaction site. The reaction rates for 1 and 2 are written as follows

$$r_1 = k_A[A]\theta_V - k_A'\theta_A \quad (3)$$

$$r_2 = k_r\theta_A \quad (4)$$

, where θ_V and θ_A are the vacant ratio and the ratio occupied by A species on the surface, and [A] is the concentration of A in the liquid phase. Assuming that the reaction rate of (3) is quick enough under an equilibrium, and defining $K_A = k_A/k_A'$ as an adsorption equilibrium constant. Since the reaction rate for the whole reaction is assumed to be r_2, and it is written in the following,

$$r_2 = \frac{k_r K_A[A]}{1 + K_A[A]} \quad (5)$$

When $K_A[A] << 1$, r_2 is approximated to be $k_r K_A[A]$, and when $K_A[A] >> 1$, it is approximated to be k_r. The latter condition was satisfied for the oxidation of BAlc, and the former was for the reduction of NB.

Acknowledgements

Notes and references

[a] Department of Applied Physics, Chuo University, 1-13-27 Kasuga, Bunkyo, Tokyo, 112-8656, Japan
[b] Graduate School of Engineering, Gunma University, 1-5-1 Tnejin-cho, Kiryu, Gunma 376-8515, Japan.

Electronic Supplementary Information (ESI) available: [Experimental setups are given in Fig.S1-S3. Examples of the fitting for the UV spectra by using the reference spectra of the reactants and products are given in Fig.S4.]. See DOI: 10.1039/b000000x/

1. N. P. Serpone, E.; Hidaka, H, *Photocatalytic Purification and Treatment of Water and Air*, Elsevier, London, 1993.
2. C. J. Li, G. R. Xu, B. H. Zhang and J. R. Gong, *Applied Catalysis B-Environmental*, 2012, **115**, 201-208.
3. P. Ciambelli, D. Sannino, V. Palma and V. Vaiano, *Catalysis Today*, 2005, **99**, 143-149.
4. K. Imamura, H. Tsukahara, K. Hamamichi, N. Seto, K. Hashimoto and H. Kominami, *Applied Catalysis A: General*, 2013, **450**, 28-33.
5. S. Yurdakal and V. Augugliaro, *Rsc Advances*, 2012, **2**, 8375-8380.

6. J. T. Carneiro, A. R. Almeida, J. A. Moulijn and G. Mul, *Physical Chemistry Chemical Physics*, 2010, **12**, 2744-2750.
7. O. S. Mohamed, A. M. Gaber and A. A. Abdel-Wahab, *Journal of Photochemistry and Photobiology a-Chemistry*, 2002, **148**, 205-210.
8. K. Imamura, T. Yoshikawa, K. Hashimoto and H. Kominami, *Applied Catalysis B: Environmental*, 2013, **134–135**, 193-197.
9. A. Maldotti, L. Andreotti, A. Molinari, S. Tollari, A. Penoni and S. Cenini, *Journal of Photochemistry and Photobiology a-Chemistry*, 2000, **133**, 129-133.
10. V. Brezová, A. Blažková, I. Šurina and B. Havlínová, *Journal of Photochemistry and Photobiology A: Chemistry*, 1997, **107**, 233-237.
11. Y. Shiraishi and T. Hirai, *Journal of Photochemistry and Photobiology C: Photochemistry Reviews*, 2008, **9**, 157-170.
12. H. Yoshida, *Photocatalytic Organic Synthesis*, Springer, New York, 2010.
13. V. VAugugliaro, T. Caronna, A. D. Paola, G. Marci, M. Pagliaro, G. Palmisano and L. Palmisano, *TiO2-Based Photocatalysis for Organic Synthesis*, Springer, New York, 2010.
14. S. O. Flores, O. Rios-Bernij, M. A. Valenzuela, I. Cordova, R. Gomez and R. Gutierrez, *Topics in Catalysis*, 2007, **44**, 507-511.
15. J. L. F. W. H. Glaze, *Langmuir*, 1998, **14**, 3551-3555.
16. O. Rios-Berny, S. O. Flores, I. Cordova and M. A. Valenzuela, *Tetrahedron Letters*, 2010, **51**, 2730-2733.
17. K. Selvam and M. Swaminathan, *Tetrahedron Letters*, 2010, **51**, 4911-4914.
18. K. Selvam and M. Swaminathan, *Catalysis Communications*, 2011, **12**, 389-393.
19. R. Abe, *Journal of Photochemistry and Photobiology C: Photochemistry Reviews*, 2010, **11**, 179-209.
20. S. I. Allakhverdiev, V. Thavasi, V. D. Kreslavski, S. K. Zharmukhamedov, V. V. Klimov, S. Ramakrishna, D. A. Los, M. Mimuro, H. Nishihara and R. Carpentier, *Journal of Photochemistry and Photobiology C: Photochemistry Reviews*, 2010, **11**, 101-113.
21. K. Maeda, *Journal of Photochemistry and Photobiology C: Photochemistry Reviews*, 2011, **12**, 237-268.
22. Y. Han, H. S. Kim and H. Kim, *Journal of Nanomaterials*, 2012, **2012**, 1-10.
23. S. I. In and R. Berg, *Asian Journal of Chemistry*, 2012, **24**, 428-432.
24. Z. Liu, X. Zhang, S. Nishimoto, T. Murakami and A. Fujishima, *Environmental Science & Technology*, 2008, **42**, 8547-8551.
25. M. Mori, K. Tanaka, H. Taoda, M. Ikedo and H. Itabashi, *Talanta*, 2006, **70**, 169-173.
26. N. Tsuchiya, K. Kuwabara, A. Hidaka, K. Oda and K. Katayama, *Physical chemistry chemical physics : PCCP*, 2012, **14**, 4734-4741.
27. N. Wang, Y. P. Zhang, L. Lei, H. L. W. Chan and X. M. Zhang, in *Nems/Mems Technology and Devices*, 2011, vol. 254, pp. 219-222.
28. Y. Matsushita, N. Ohba, S. Kumada, T. Suzuki and T. Ichimura, *Catalysis Communications*, 2007, **8**, 2194-2197.
29. Y. Matsushita, M. Iwasawa, T. Suzuki and T. Ichimura, *Chemistry Letters*, 2009, **38**, 846-847.
30. Y. Matsushita, S. Kumada, K. Wakabayashi, K. Sakeda and T. Ichimura, *Chemistry Letters*, 2006, **35**, 410-411.
31. R. Gorges, S. Meyer and G. Keisel, *J. Photochem. Photobio. A*, 2004, **167**, 95-99.
32. E. E. Coyle and M. Oelgemoller, *Photochemical & Photobiological Sciences*, 2008, **7**, 1313-1322.
33. N. M. Mahmoodi, M. Arami, N. Y. Limaee and N. S. Tabrizi, *Chemical Engineering Journal*, 2005, **112**, 191-196.
34. I. K. Konstantinou and T. A. Albanis, *Applied Catalysis B: Environmental*, 2004, **49**, 1-14.
35. K. Katayama, Y. Takeda, K. Kuwabara and S. Kuwahara, *Chemical Communications*, 2012, **48**, 7368-7370.
36. A. Mase, T. Sugita, M. Mori, S. Iwamoto, T. Tokutome, K. Katayama and H. Itabashi, *Chemical Engineering Journal*, 2013, **225**, 440-446.
37. A. Maldotti and A. Molinari, in *Photocatalysis*, 2011, vol. 303, pp. 185-216.
38. A. I. Kryukov, S. Y. Kuchmy, S. V. Kulik and A. V. Korzhak, *Teoreticheskaya I Eksperimentalnaya Khimiya*, 1992, **28**, 416-419.

Table of Content

Methodology to understand the ability of photocatalytic materials. Conversion of simple organic molecules was monitored in-situ in photocatalytic microreactors.